Chemical Science

ROYAL SOCIETY OF CHEMISTRY

EDGE ARTICLE

View Article Online
View Journal | View Issue

Cite this: *Chem. Sci.*, 2025, **16**, 13449

All publication charges for this article have been paid for by the Royal Society of Chemistry

Received 11th April 2025
Accepted 12th June 2025

DOI: 10.1039/d5sc02695d

rsc.li/chemical-science

Nickel-catalyzed diastereoselective hydroboration of acrylates with a vinylborane reagent†

Guanwen Hu, Peiqi Zhang, Xinmou Wang, Chunteng Wan, Yiyi Fu, Wa Hung Leung, Zhenyang Lin * and Yangjian Quan *

Organoboron compounds exhibit unique properties and valuable applications in organic synthesis, catalysis, materials science, and drug discovery, driving researchers to improve their structural and functional diversity. Despite significant advancements, challenges remain in accessing complex organoboron compounds, particularly in constructing boron-stereogenic skeletons. Here we report a nickel catalyzed diastereoselective hydroboration of olefins using a newly developed vinylborane reagent, CH_2=CH–BH_2L (where L is a dative donor). This protocol enables the efficient synthesis of versatile vinylborane derivatives featuring a boron-stereogenic center. Mechanistic studies, including the isolation and structural characterization of a key B–H–Ni bonded intermediate, control experiments, and DFT calculations reveal a σ-coordination enabled B(sp^3)–H activation. The σ-coordination induces an oxidative metalation, simultaneously forming B–Ni, C–Ni and C–H bonds. The C=C unit in the vinylborane reagent plays a pivotal role in facilitating the otherwise challenging oxidative metalation of the B(sp^3)–H bond. This unique B(sp^3)–H metalation mode may have broader implications for achieving other forms of selective B–H functionalization.

Introduction

Organoboron compounds are finding increasingly valuable applications in synthetic chemistry, materials science, and drug discovery. Notably, due to the unique interactions between borane motifs and bioactive centers, five boron-based drugs have been approved by the FDA, and more candidates are under clinical trials (Fig. 1a).[1–3] Furthermore, boron-containing units such as azaborines[4–6] and carboranes[7,8] serve as benzene analogues to enhance or alter the bioactivity of the lead drug molecules. Given these advancements, it remains a compelling goal to enhance the structural and functional complexity of organoboron molecules. Despite significant progress, challenges persist in the synthesis of complex organoboranes, particularly in constructing boron-stereogenic skeletons.[9,10] To address these challenges and expand the chemical space of organoboranes, design and development of a versatile reagent would be an ideal solution.

In view of the inherent versatility of C=C and C–B units, vinylboron reagents containing both active centers have been developed and proven to be powerful synthons for organoborane synthesis and organic transformations (Fig. 1b).[11–19] These reagents typically undergo three main reaction modes, including (1) C=C double bond modifications,[20–30] (2) C–B bond transformations,[13,31–34] and (3) 1,2-migrations of "boron-ate" complexes.[35–39] However, functionalization at the boron center assisted by the C=C motif in vinylboron reagents remains unexplored, despite its potential to access boron-stereogenic compounds. In this connection, we have designed a bench-stable vinylborane reagent, CH_2=CH–BH_2L (**1**, L is a dative donor). This reagent is hypothesized to undergo B(sp^3)–H functionalization to generate a broad range of vinylborane derivatives distinguished by a chiral-at-boron center (Fig. 1b).[9,10,40–44] For realizing effective B(sp^3)–H modification, the activation strategy should be able to differentiate the B(sp^3)–H site from other active centers in **1** and allow for precise selectivity control.

A promising approach for selective B–H derivatization involves transition metal catalysis,[45–52] which has been widely applied in borylative transformations[53–65] but remains relatively underdeveloped in B(sp^3)–H activation.[66–68] Pioneering studies by Weller,[69] Chuzel and Parrain,[43] and Shi[70] demonstrated noble metal catalysts (*e.g.*, Rh, Au) for B(sp^3)–H functionalization, but successful examples remain scarce. This difficulty arises because B(sp^3)–H bonds are electron-rich, weakly polarized, and lack an empty p-orbital on boron, making their oxidative addition on transition metals challenging compared to B(sp^2)–H bonds. Interestingly, several studies document σ-coordination of B(sp^3)–H bonds to transition metal centers, which weakens the B(sp^3)–H bond and may facilitate its activation.[71–75] Building on this premise, we have developed a nickel-catalyzed

Department of Chemistry, The Hong Kong University of Science and Technology, Clear Water Bay, Kowloon, Hong Kong SAR, China. E-mail: chzlin@ust.hk; chyjquan@ust.hk

† Electronic supplementary information (ESI) available. CCDC 2381595, 2381592 and 2381593. For ESI and crystallographic data in CIF or other electronic format see DOI: https://doi.org/10.1039/d5sc02695d

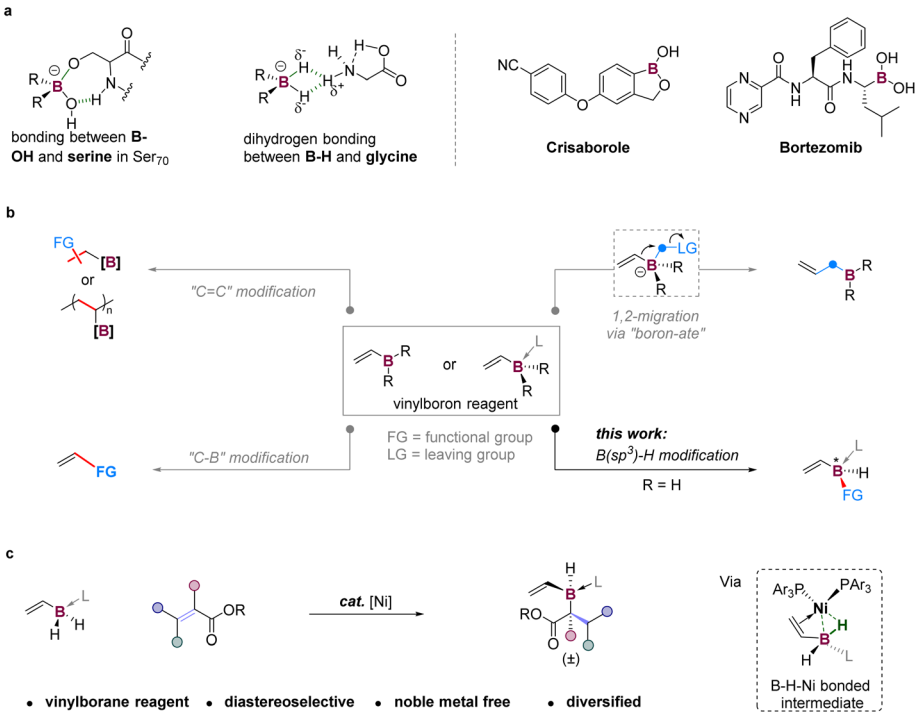

Fig. 1 Vinylborane reagent. (a) Unique interactions between boron motifs and biomolecules, and representative FDA-approved boron drugs. (b) Representative reaction modes of vinylboron reagents and the unexplored B(sp^3)–H functionalization. (c) This work: design of a vinylborane reagent and its reaction with olefins *via* nickel catalysis.

diastereoselective hydroboration of olefins using the vinylborane reagent (Fig. 1c). The successful isolation and structural characterization of a key B–H–Ni bonded intermediate, along with control experiments and DFT calculations, reveal a unique σ-coordination enabled oxidative metalation that simultaneously generates B–Ni, C–Ni and C–H bonds while cleaving the B–H bond and olefin π bond. The C=C unit in the vinylborane reagent plays a crucial role in facilitating the key oxidative metalation of the B(sp^3)–H bond.

Results and discussion

In the presence of $NiBr_2(PPh_3)_2$ as a catalyst, reaction of the vinylborane reagent **1** with benzyl acrylate in dioxane at room temperature overnight gave the coupling product **3** in 80% yield with a diastereomeric ratio (d_r) of 8 : 1 (entry 1, Table 1). Using $NiCl_2$ as the catalyst without a phosphine ligand provided a comparable yield of 75%, but with a significantly reduced d_r of 1.1 : 1 (entry 2, Table 1). We then screened a series of ligands to improve the d_r of product **3** (Table 1 and S1b in the ESI†). Monophosphine ligands, P(*p*-F–Ph)$_3$ and P(*p*-Cl–Ph)$_3$, proved optimal, leading to excellent d_{rs} of > 20 : 1. The most electron-deficient $P(C_6F_5)_3$, electron-rich PCy_3, or bidentate phosphine ligands offered low d_{rs} ranging from 1 : 1 to 2 : 1 (entries 7 and 9, Tables 1 and S1b in the ESI†). Using less polar toluene as the solvent increased the yield to 97% without compromising the d_r (entry 12, Table 1). The employment of $Ni(COD)_2$ instead of $NiCl_2$ resulted in a decreased yield of 84% with a reduced d_r of 16 : 1 (entry 13, Table 1). Reducing the loadings of $NiCl_2$ and P(*p*-F–Ph)$_3$ to 5 mol% and 12.5 mol%, respectively, did not affect the reaction efficiency (entry 14, Table 1) and was therefore chosen as the optimal reaction condition. Replacing the vinylborane reagent **1** with NHC–BH_3 or NHC–BH_2Ph failed to give the target product (Section 4.4 in the ESI†), highlighting the important role of the "C=C" motif in **1** in facilitating B–H metalation/activation. In contrast, the previously developed boryl radical strategy proved to give β-borylation products with poor diastereoselectivity (Fig. S14†).[66,76–80]

To gain insights into the reaction mechanism, control experiments were conducted. Treatment of **1**, $Ni(COD)_2$, and P(*p*-F–Ph)$_3$ in THF at room temperature for 6 h produced a B–H–Ni bonded complex **INT1** in 60% isolated yield (Fig. 2a). The ^{1}H NMR spectrum of **INT1** exhibited a significantly up-field peak at −0.88 ppm (Fig. 2c). Its assignment to one BH was supported by the subsequent ^{11}B–^{1}H HSQC analysis, with another BH being detected at 0.66 ppm (Fig. 2c). The B(sp^3)–H coordination mode was further verified by the single-crystal structure of **INT1** (Fig. 2a). Upon hydrogen addition through modeling, the bond length of the B(sp^3)–H σ-coordinated to the Ni center was measured as 1.29 Å, longer than the 1.13 Å length measured for the free B(sp^3)–H bond. Moreover, the distance between the B and Ni centers was found to be 2.28 Å, suggesting a potential interaction. A combination of the NMR and X-ray diffraction findings indicated (1) the σ-coordination of one B(sp^3)–H in the vinylborane reagent to the Ni center and (2) the significant activation of this B(sp^3)–H bond by Ni. Such a bonding and activation mode differs from the deprotonation or C–H metalation reaction observed in forming transition metal-allylic

Table 1 Synthesis of **1** and optimization of reaction conditions[a]

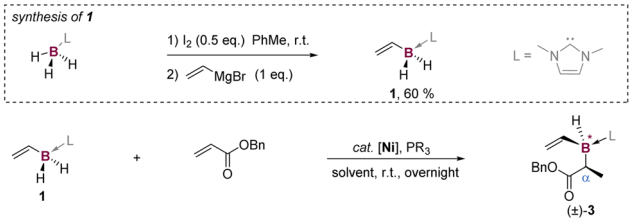

Entry	[Ni] (10 mol%)	PR_3 (25 mol%)	Solvent	Yield[b] (%)	d_r[b]
1	$NiBr_2(PPh_3)_2$	—	Dioxane	80	8/1
2	$NiCl_2$	—	Dioxane	75	1.1/1
3	$NiCl_2$	PPh_3	Dioxane	88	19/1
4	$NiCl_2$	P(*p*-F–Ph)$_3$	Dioxane	92	>20/1
5	$NiCl_2$	P(*p*-Cl–Ph)$_3$	Dioxane	88	>20/1
6	$NiCl_2$	P(*p*-OMe–Ph)$_3$	Dioxane	89	18/1
7	$NiCl_2$	$P(C_6F_5)_3$	Dioxane	72	1.1/1
8	$NiCl_2$	P(*p*-Me–Ph)$_3$	Dioxane	91	12/1
9	$NiCl_2$	PCy_3	Dioxane	42	2/1
10	$NiCl_2$	P(*p*-F–Ph)$_3$	MeCN	37	11/1
11	$NiCl_2$	P(*p*-F–Ph)$_3$	DMA	87	14/1
12	$NiCl_2$	P(*p*-F–Ph)$_3$	Toluene	>95	>20/1
13	$Ni(COD)_2$	P(*p*-F–Ph)$_3$	Toluene	84	16/1
14	**$NiCl_2$**	**P(*p*-F–Ph)$_3$**[c]	**Toluene**	**>95 (97)**	**>20/1**

[a] Reactions were conducted at 0.05 mmol scale in 0.5 mL of solvent in a closed flask. [b] Yields and d_{rs} were determined by ^{1}H NMR with 1,3,5-trimethoxybenzene as an internal standard. [c] 5 mol% $NiCl_2$ and 12.5 mol% P(*p*-F–Ph)$_3$ were used, isolated yield in parentheses.

complexes,[81,82] probably due to the distinct electronic nature of B(sp^3)–H (hydridic) *versus* C–H (protonic). Compound **INT1** reacted with ethyl (*E*)-2-hexenoate under the standard conditions to deliver **41** in 21% yield with a d_r of over 20 : 1 (Fig. 2b). It was also proved effective as a catalyst in the hydroboration reaction (Fig. 2b). These results support the role of **INT1** as a key intermediate involved in the reaction pathway.

DFT calculations were carried out to gain insight into the reaction mechanism. Fig. 2g shows the energy profile calculated. Starting from **INT1** (using its single crystal structure for geometry optimization), a ligand substitution of benzyl acrylate for P(*p*-F–Ph)$_3$ leads to the formation of **INT2**, from which the crucial oxidative metalation occurs, establishing B–Ni, C–Ni, and C–H bonds in **INT3** concurrently, while cleaving a B–H bond and benzyl acrylate π bond. The energy barrier for this metalation step is 19.9 kcal mol^{-1}, being the highest in the calculated pathway (Fig. 2g). Subsequently, **INT3** undergoes reductive elimination, followed by product release to deliver the final product and regenerate **INT1**. Diastereoselectivity control is closely associated with the rate-determining step. Therefore, optimization was conducted for the four diastereomers of **TS1**, originating from three chiral B, Ni, and C (bonded with the ester group) centers (Fig. S15 in the ESI†). Among them, the diastereomer with the least steric repulsion between the olefin substrate and the phosphine ligand was most favored (Fig. 2g), leading to product **3** with a configuration identical to experimental observations (see single crystal structures of **4** and **21** in Fig. 3).

The deuterated vinylborane reagent **1-*D*** was prepared and reacted with 2-furanone to yield **49-*D***, wherein one hydrogen of the β-CH_2, with respect to boron, was deuterated at a rate of 67% (Fig. 2d). The addition of 1.5 equiv. of D_2O into the reaction mixture did not cause any B–H or C–H deuteration (Fig. 2d). Competitive and parallel experiments using **1** and **1-*D*** displayed significant kinetic isotope effect (KIE) with k_H/k_D ratios of 2.5 and 2.4, respectively (Fig. 2e). These experimental findings suggested that the B(sp^3)–H cleavage might be involved in the rate-determining step, consistent with the computational results. Based on the above experiments and DFT calculations, a plausible reaction pathway is proposed in Fig. 2f.

The reaction mode of B(sp^3)–H metalation is very similar to the documented ligand-to-ligand hydrogen transfer (LLHT) mechanism observed in C(sp^2)–H nickelation.[83,84] The difference lies in the bond strength between Ni–B(sp^3) and Ni–C(sp^2). The former one is believed to be relatively weak due to the lack of π-interaction between metal and the boron unit.[85] Therefore, its formation *via* LLHT is involved in the rate-determining step.

We then explored the scope of various types of olefins. Terminal vinyl esters containing a diverse array of functional groups, including alkyl, trifluoromethyl, alkenyl, alkynyl, cyano, methoxyl, ether, halide, silyl, carbonyl, amide, ester, bpin, and pyridinyl groups, reacted with the vinylborane reagent smoothly (**3–29**, Fig. 3). Most reactions exhibited excellent diastereomeric ratios of >20 : 1. Notably, carbonyl and pyridinyl substituents, which can coordinate to nickel, were well tolerated (**21** and **29**). The hydroboration occurred regioselectively at the relatively electron-poor C=C site, when the substrates involved multiple unsaturated functionalities (**10–14**). The ferrocene-containing substrate worked well (**30**), while the cyclobutylamino substituent proved compatible (**31**). A series of aryl acrylates were evaluated, giving **32–38** in moderate to excellent isolated yields, yet with relatively low diastereomeric ratios of around 10 : 1. Alkyl thioacrylate was also an effective coupling partner, delivering product **39**.

A series of internal olefins were subsequently evaluated as substrates. Various functional groups including piperidine, tetrahydropyrane, nerolin, and phthalimide were well tolerated (**42–45**). The substrate featuring a cyclopropylethene motif underwent this hydroboration effectively to afford **46**, where the cyclopropyl ring remained intact, negating the involvement of a radical pathway. In addition to 1,2-disubstituted olefins, the 1,1′-disubstituted one also worked well (**50**), constructing a quaternary C–B(sp^3) bond. Tri-substituted olefins afforded the corresponding products (**51**, **53–55**) effectively, albeit with compromised diastereomeric ratios. However, the tetra-substituted olefin failed to react with the vinylborane reagent **1** (Section 4.4 in the ESI†). These results imply the influence of steric factors on the reaction efficiency and diastereoselectivity. Less bulky cyclic olefins were compatible, yielding **49** and **52** with diastereomeric ratios of >20 : 1.

This protocol also enabled the straightforward introduction of a versatile vinylborane motif into a broad array of bioactive molecules, including derivatives of commercially available

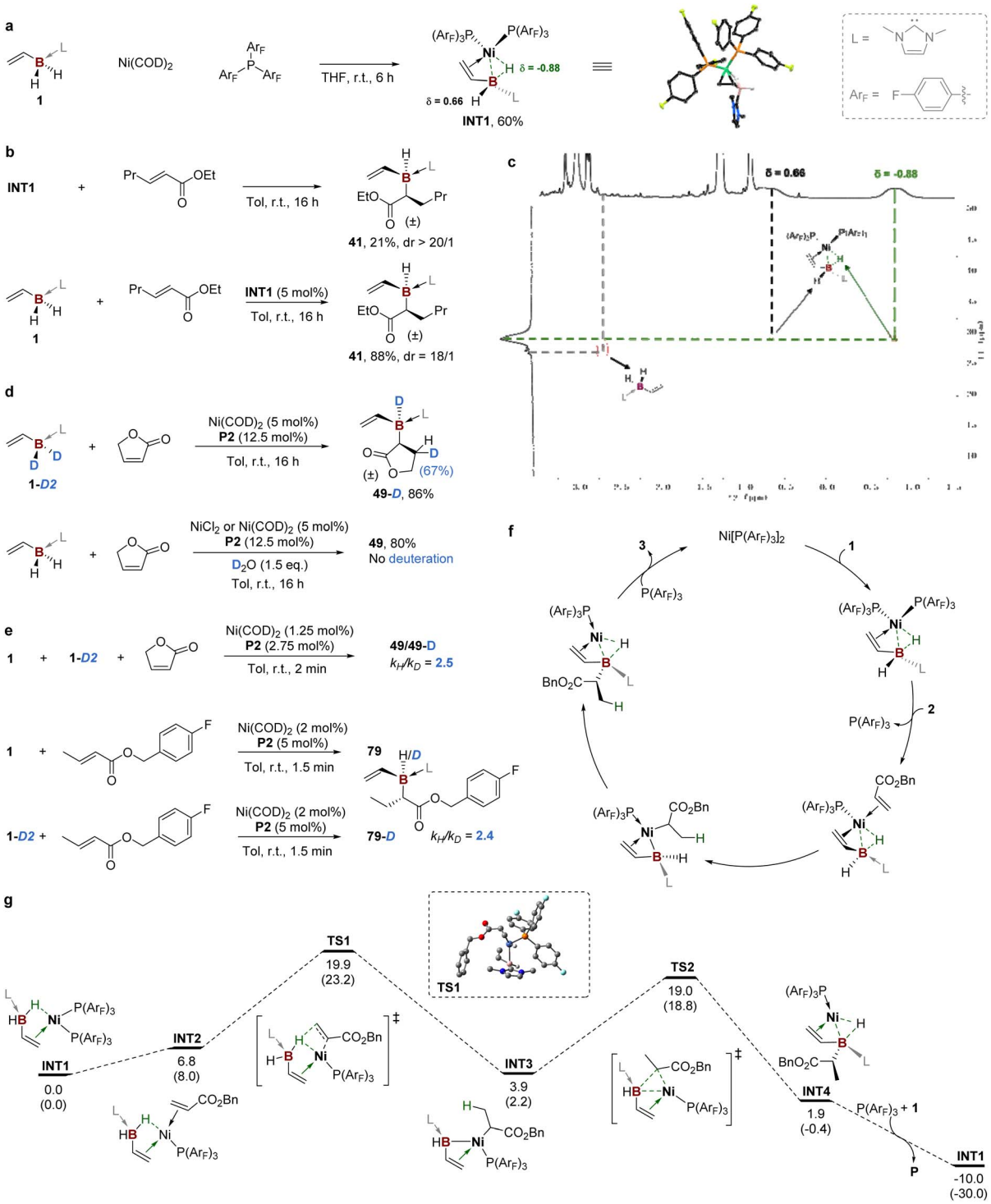

Fig. 2 Mechanistic investigations. (a) Synthesis and single crystal structure of **INT1**. (b) Demonstrating the role of **INT1** in catalytic hydroboration. (c) $^{1}H-^{11}B$ HMQC spectrum of **INT1**. (d) Deuterium labelling experiments. (e) KIE determination experiments. (f) Proposed reaction mechanism. (g) DFT calculations on B3LYP-D3(BJ)/def2-QZVPP (Ni), def2-TZVP (rest)/SMD (toluene)//B3LYP-D3(BJ)/def2-TZVP (Ni, P), 6-31G(d,p) (rest)/PCM (toluene) level; relative Gibbs free energies and relative electronic energies (in parentheses) in kcal mol^{-1}.

medicines (Fig. 4a): diclofenac (**61**, anti-inflammatory), probenecid (**62**, for treating gout and hyperuricemia), febuxostat (**63**, for treating gout), telmisartan (**66**, for treating high blood pressure, heart failure, and diabetic nephropathy), ciprofibrate (**68**, a hypolipidemic agent), and indometacin (**65** and **67**, anti-inflammatory). Additionally, cholesterol (**64**), estrone (**60**), Boc-Ser-OMe (**59**, an amino acid), diacetone-D-glucose (**58**, a pharmaceutical intermediate), menthol (**57**, anti-

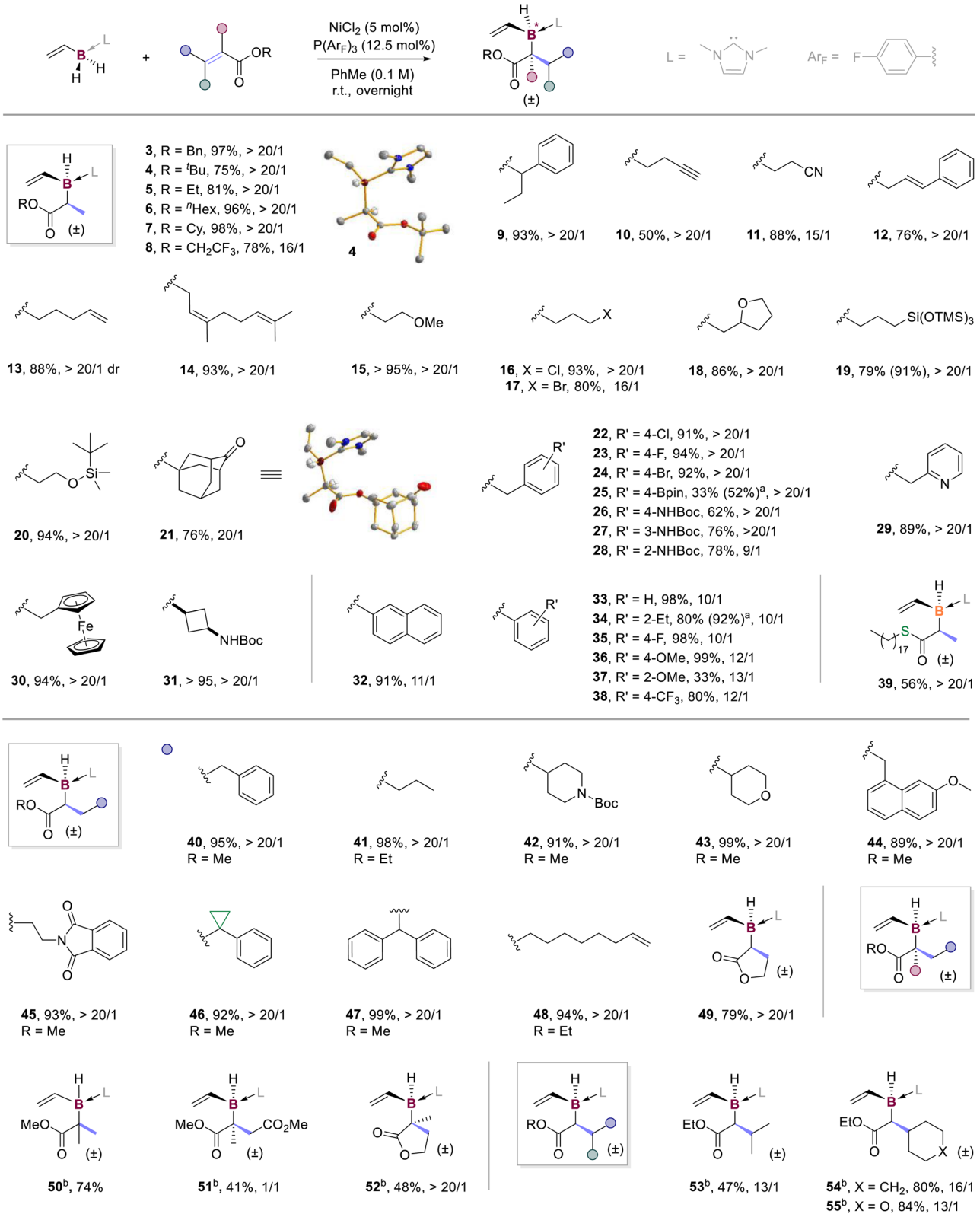

Fig. 3 Substrate scope. Reaction conditions: $NiCl_2$ (5 mol%), P(*p*-F–Ph)$_3$ (12.5 mol%), **1** (0.12 mmol), alkene (0.1 mmol), PhMe (1 mL), r.t., 16 h; yields of isolated products. (a) ^{1}H NMR yields are shown in parentheses. (b) Reaction conditions: $Ni(COD)_2$ (10 mol%), P(*p*-F–Ph)$_3$ (25 mol%), **1** (0.12 mmol), alkene (0.1 mmol), PhMe (1 mL), r.t., 16 h.

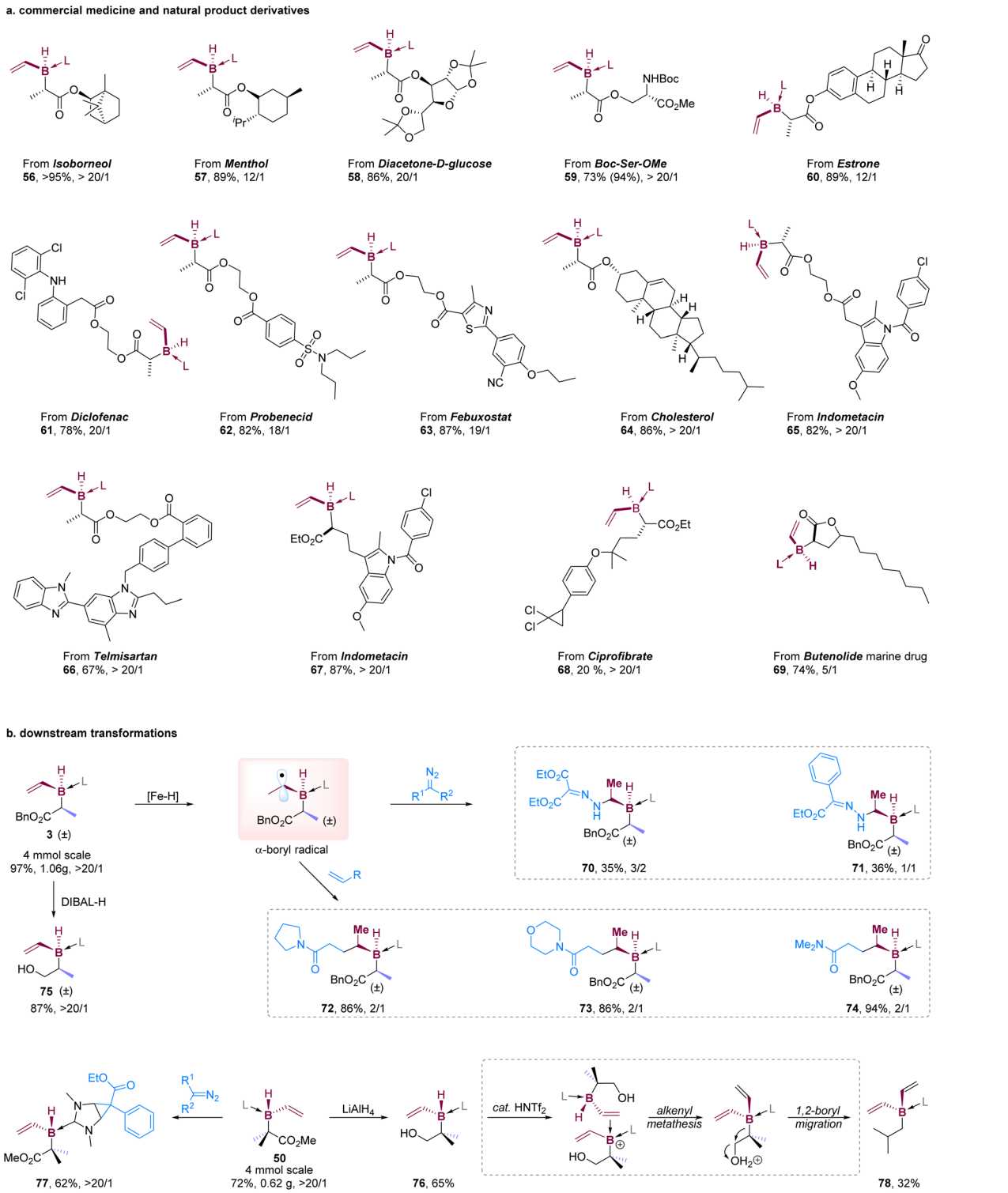

Fig. 4 Derivatization and synthetic applications. (a) Integrating the vinylborane motif into commercial medicine and natural product derivatives. (b) Large-scale synthesis and downstream transformations of the products.

irritation), isoborneol (**56**, antiviral), and butenolide (**69**, a marine drug) derivatives reacted well with the vinylborane reagent, achieving good to excellent diastereomeric ratios. These findings highlight the remarkable compatibility and promising potential of this nickel-catalytic protocol.

This nickel-catalyzed hydroboration was conveniently scaled up to give **3** and **50** in 97% and 72% yields, respectively (Fig. 4b). The introduced vinylborane motif is anticipated to be versatile for further molecular modifications, alike the previously reported vinylboron fragments. Treatment of **3** with *in situ* generated [Fe]–H species[86,87] delivered a new α-boryl(sp^3)

radical, which effectively attacked olefins or diazo compounds to give **72–74** and **70–71**, respectively. The ester groups in **3** and **50** were conveniently reduced to give **75** and **76**. Attempts to construct a four-membered oxaboracycle from **76** *via* Brønsted acid catalyzed B–H/O–H dehydrogenative coupling failed. However, an unexpected product **78** was isolated and characterized (see Fig. S3 in the ESI†). A plausible pathway including a sequence of borenium-induced alkenyl metathesis, nucleophilic 1,2-boryl shift, and carbocation hydridation was proposed accordingly (see Fig. 4b and S4 in the ESI†). Reaction of **50** with the diazo compound upon visible light irradiation yielded **77** bearing a bicyclo[3.1.0] ring,[62] rather than the B–H insertion species.[58]

Conclusions

In summary, we have designed a new vinylborane reagent that permits the facile modification at the boron center *via* B(sp^3)–H bond functionalization. The developed nickel catalytic protocol demonstrates advantages of remarkable diastereoselectivity control, good compatibility, and mild operation conditions. The isolation and structural characterization of a B–H–Ni bonded intermediate, along with DFT calculations, underscore the important bidentate coordination of the vinylborane reagent to the nickel center. This coordination induces a unique oxidative metalation, distinct from the metalation modes observed for allylic C–H bonds. The potential of this vinylborane reagent in synthetic chemistry awaits further research efforts.

Data availability

Crystallographic data for **INT1**, 4, 21 have been deposited at the CCDC under 2381595, 2381592, 2381593 and can be obtained from **https://www.ccdc.cam.ac.uk/**. Detailed synthetic procedures, characterization of boranes, and mechanistic investigations supporting this article have been uploaded as ESI.†

Author contributions

G. H., X. W., and Y. Q. conceived and designed the experiments. G. H., P. Z., X. W., C. W., and Y. F. performed experiments. C. W. and W. H. L. performed crystallization and structural resolution. P. Z. and Z. L. performed DFT calculations. G. H., P. Z., Z. L., and Y. Q. wrote the manuscript. Z. L. and Y. Q. directed the research.

Conflicts of interest

There are no conflicts to declare.

Acknowledgements

The authors acknowledge the start-up funding (Project No. R9804 to Y. Q.) from the Hong Kong University of Science and Technology (HKUST), Early Career Scheme from the Research Grants Council of Hong Kong (Project Number: 26307123 to Y. Q.), NSFC Young Scholar Fund (Project Number: NSFC23SC02 to Y. Q.), and the General Research Fund from the Research Grants Council of Hong Kong (HKUST 16302222 to Z. L.). Dr Herman Ho-Yung SUNG and Prof. Dr Ian Williams are acknowledged for X-ray crystallography. Dr Yu CAO, Prof. Dr Wan CHAN and Ms. Wing-Laam LUK are acknowledged for HRMS test.

Notes and references

1 R. J. Grams, W. L. Santos, I. R. Scorei, A. Abad-García, C. A. Rosenblum, A. Bita, H. Cerecetto, C. Viñas and M. A. Soriano-Ursúa, The Rise of Boron-Containing Compounds: Advancements in Synthesis, Medicinal Chemistry, and Emerging Pharmacology, *Chem. Rev.*, 2024, **124**, 2441–2511.
2 S. X. Tian, H.-B. Li and J. Yang, Monoanion BH4− Can Stabilize Zwitterionic Glycine with Dihydrogen Bonds, *ChemPhysChem*, 2009, **10**, 1435–1437.
3 A. Prester, M. Perbandt, M. Galchenkova, D. Oberthuer, N. Werner, A. Henkel, J. Maracke, O. Yefanov, J. Hakanpää, G. Pompidor, J. Meyer, H. Chapman, M. Aepfelbacher, W. Hinrichs, H. Rohde and C. Betzel, Time-resolved crystallography of boric acid binding to the active site serine of the β-lactamase CTX-M-14 and subsequent 1,2-diol esterification, *Commun. Chem.*, 2024, **7**, 152.
4 Z. X. Giustra and S.-Y. Liu, The State of the Art in Azaborine Chemistry: New Synthetic Methods and Applications, *J. Am. Chem. Soc.*, 2018, **140**, 1184–1194.
5 A. Bhattacharjee, G. H. M. Davies, B. Saeednia, S. R. Wisniewski and G. A. Molander, Selectivity in the Elaboration of Bicyclic Borazarenes, *Adv. Synth. Catal.*, 2021, **363**, 2256–2273.
6 J. J. Blackner, O. M. Schneider, W. O. Wong and D. G. Hall, Removing Neighboring Ring Influence in Monocyclic B–OH Diazaborines: Properties and Reactivity as Phenolic Bioisosteres with Dynamic Hydroxy Exchange, *J. Am. Chem. Soc.*, 2024, **146**, 19499–19508.
7 P. Stockmann, M. Gozzi, R. Kuhnert, M. B. Sárosi and E. Hey-Hawkins, New keys for old locks: carborane-containing drugs as platforms for mechanism-based therapies, *Chem. Soc. Rev.*, 2019, **48**, 3497–3512.
8 A. Marfavi, P. Kavianpour and L. M. Rendina, Carboranes in drug discovery, chemical biology and molecular imaging, *Nat. Rev. Chem.*, 2022, **6**, 486–504.
9 A. Abdou-Mohamed, C. Aupic, C. Fournet, J.-L. Parrain, G. Chouraqui and O. Chuzel, Stereoselective formation of boron-stereogenic organoboron derivatives, *Chem. Soc. Rev.*, 2023, **52**, 4381–4391.
10 X. Li, G. Zhang and Q. Song, Recent advances in the construction of tetracoordinate boron compounds, *Chem. Commun.*, 2023, **59**, 3812–3820.
11 Y.-L. Feng, B.-W. Zhang, Y. Xu, S. Jin, D. Mazzarella and Z.-Y. Cao, The reactivity of alkenyl boron reagents in catalytic reactions: recent advances and perspectives, *Org. Chem. Front.*, 2024, **11**, 7249–7277.

12 J. Carreras, A. Caballero and P. J. Perez, Alkenyl Boronates: Synthesis and Applications, *Chem Asian J.*, 2019, **14**, 329–343.
13 G. A. Molander and N. Ellis, Organotrifluoroborates: protected boronic acids that expand the versatility of the Suzuki coupling reaction, *Acc. Chem. Res.*, 2007, **40**, 275–286.
14 T. Nishikawa, Radical polymerization of alkenyl boronates and C–B bond transformation: polymer synthesis through side-chain replacement for overcoming synthetic limitations, *Polym. J.*, 2024, **56**, 873–886.
15 B. E. Uno, E. P. Gillis and M. D. Burke, Vinyl MIDA boronate: a readily accessible and highly versatile building block for small molecule synthesis, *Tetrahedron*, 2009, **65**, 3130–3138.
16 C. Jiang and D. W. Stephan, Hydrophosphination of vinylboranes with phosphinoamines, *Dalton Trans.*, 2013, **42**, 3318–3325.
17 V. Fasano, J. Cid, R. J. Procter, E. Ross and M. J. Ingleson, Selective Boryl-Anion Migration in a Vinyl sp(2) -sp(3) Diborane Induced by Soft Borane Lewis Acids, *Angew. Chem., Int. Ed.*, 2018, **57**, 13293–13297.
18 M. Shimoi, T. Watanabe, K. Maeda, D. P. Curran and T. Taniguchi, Radical trans-Hydroboration of Alkynes with N-Heterocyclic Carbene Boranes, *Angew. Chem., Int. Ed.*, 2018, **57**, 9485–9490.
19 A. Marotta, C. E. Adams and J. J. Molloy, The Impact of Boron Hybridisation on Photocatalytic Processes, *Angew. Chem., Int. Ed.*, 2022, **61**, e202207067.
20 K. Sasaki and T. Hayashi, Rhodium-catalyzed asymmetric conjugate addition of arylboroxines to borylalkenes: asymmetric synthesis of beta-arylalkylboranes, *Angew. Chem., Int. Ed.*, 2010, **49**, 8145–8147.
21 J. Carreras, A. Caballero and P. J. Perez, Enantio- and Diastereoselective Cyclopropanation of 1-Alkenylboronates: Synthesis of 1-Boryl-2,3-Disubstituted Cyclopropanes, *Angew. Chem., Int. Ed.*, 2018, **57**, 2334–2338.
22 A. Noble, R. S. Mega, D. Pflasterer, E. L. Myers and V. K. Aggarwal, Visible-Light-Mediated Decarboxylative Radical Additions to Vinyl Boronic Esters: Rapid Access to gamma-Amino Boronic Esters, *Angew. Chem., Int. Ed.*, 2018, **57**, 2155–2159.
23 J. Levi Knippel, A. Z. Ni, A. W. Schuppe and S. L. Buchwald, A General Strategy for the Asymmetric Preparation of alpha-Stereogenic Allyl Silanes, Germanes, and Boronate Esters *via* Dual Copper Hydride- and Palladium-Catalysis, *Angew. Chem., Int. Ed.*, 2022, **61**, e202212630.
24 J. C. Lee, R. McDonald and D. G. Hall, Enantioselective preparation and chemoselective cross-coupling of 1,1-diboron compounds, *Nat. Chem.*, 2011, **3**, 894–899.
25 S. Bera, C. Fan and X. Hu, Enantio- and diastereoselective construction of vicinal C(sp^3) centres *via* nickel-catalysed hydroalkylation of alkenes, *Nat. Catal.*, 2022, **5**, 1180–1187.
26 L. Liu, M. C. Aguilera, W. Lee, C. R. Youshaw, M. L. Neidig and O. Gutierrez, General method for iron-catalyzed multicomponent radical cascades-cross-couplings, *Science*, 2021, **374**, 432–439.
27 M. L. Lepage, S. Lai, N. Peressin, R. Hadjerci, B. O. Patrick and D. M. Perrin, Direct Access to MIDA Acylboronates through Mild Oxidation of MIDA Vinylboronates, *Angew. Chem., Int. Ed.*, 2017, **56**, 15257–15261.
28 Y. F. Zeng, W. W. Ji, W. X. Lv, Y. Chen, D. H. Tan, Q. Li and H. Wang, Stereoselective Direct Chlorination of Alkenyl MIDA Boronates: Divergent Synthesis of E and Z alpha-Chloroalkenyl Boronates, *Angew. Chem., Int. Ed.*, 2017, **56**, 14707–14711.
29 J. J. Molloy, M. Schäfer, M. Wienhold, T. Morack, C. G. Daniliuc and R. Gilmour, Boron-enabled geometric isomerization of alkenes *via* selective energy-transfer catalysis, *Science*, 2020, **369**, 302–306.
30 N. Hanania, N. Eghbarieh and A. Masarwa, PolyBorylated Alkenes as Energy-Transfer Reactive Groups: Access to Multi-Borylated Cyclobutanes Combined with Hydrogen Atom Transfer Event, *Angew. Chem., Int. Ed.*, 2024, **63**, e202405898.
31 S. Liao, A. Porta, X. Cheng, X. Ma, G. Zanoni and L. Zhang, Bifunctional Ligand Enables Efficient Gold-Catalyzed Hydroalkenylation of Propargylic Alcohol, *Angew. Chem., Int. Ed.*, 2018, **57**, 8250–8254.
32 A. J. Lennox and G. C. Lloyd-Jones, Selection of boron reagents for Suzuki-Miyaura coupling, *Chem. Soc. Rev.*, 2014, **43**, 412–443.
33 H. Kim and D. W. MacMillan, Enantioselective organo-SOMO catalysis: the alpha-vinylation of aldehydes, *J. Am. Chem. Soc.*, 2008, **130**, 398–399.
34 Z. He and A. K. Yudin, Amphoteric alpha-boryl aldehydes, *J. Am. Chem. Soc.*, 2011, **133**, 13770–13773.
35 S. Namirembe and J. P. Morken, Reactions of organoboron compounds enabled by catalyst-promoted metalate shifts, *Chem. Soc. Rev.*, 2019, **48**, 3464–3474.
36 M. Silvi, C. Sandford and V. K. Aggarwal, Merging Photoredox with 1,2-Metallate Rearrangements: The Photochemical Alkylation of Vinyl Boronate Complexes, *J. Am. Chem. Soc.*, 2017, **139**, 5736–5739.
37 L. Zhang, G. J. Lovinger, E. K. Edelstein, A. A. Szymaniak, M. P. Chierchia and J. P. Morken, Catalytic conjunctive cross-coupling enabled by metal-induced metallate rearrangement, *Science*, 2016, **351**, 70–74.
38 M. Kischkewitz, K. Okamoto, C. Mück-Lichtenfeld and A. Studer, Radical-polar crossover reactions of vinylboron ate complexes, *Science*, 2017, **355**, 936–938.
39 H. Wang, C. Jing, A. Noble and V. K. Aggarwal, Stereospecific 1,2-Migrations of Boronate Complexes Induced by Electrophiles, *Angew. Chem., Int. Ed.*, 2020, **59**, 16859–16872.
40 C. Aupic, A. Abdou Mohamed, C. Figliola, P. Nava, B. Tuccio, G. Chouraqui, J.-L. Parrain and O. Chuzel, Highly diastereoselective preparation of chiral NHC-boranes stereogenic at the boron atom, *Chem. Sci.*, 2019, **10**, 6524–6530.
41 B. Zu, Y. Guo and C. He, Catalytic EnantioselectivConstruction of Chiroptical Boron-Stereogenic Compounds, *J. Am. Chem. Soc.*, 2021, **143**, 16302–16310.
42 G. Zhang, Z. Zhang, M. Hou, X. Cai, K. Yang, P. Yu and Q. Song, Construction of boron-stereogenic compounds *via*

enantioselective Cu-catalyzed desymmetric B–H bond insertion reaction, *Nat. Commun.*, 2022, **13**, 2624.

43 M. Toure, O. Chuzel and J.-L. Parrain, Asymmetric Rhodium-Directed anti-Markovnikov Regioselective Boracyclopentannulation, *J. Am. Chem. Soc.*, 2012, **134**, 17892–17895.

44 N. M. Ankudinov, N. V. Alexeev, E. S. Podyacheva, D. A. Chusov, K. A. Lyssenko and D. S. Perekalin, Catalytic insertion of nitrenes into B–H bonds, *Chem. Sci.*, 2025, **16**, 6298–6306.

45 D. A. Evans and G. C. Fu, Amide-directed, iridium-catalyzed hydroboration of olefins: documentation of regio- and stereochemical control in cyclic and acyclic systems, *J. Am. Chem. Soc.*, 1991, **113**, 4042–4043.

46 J. F. Hartwig, K. S. Cook, M. Hapke, C. D. Incarvito, Y. Fan, C. E. Webster and M. B. Hall, Rhodium Boryl Complexes in the Catalytic, Terminal Functionalization of Alkanes, *J. Am. Chem. Soc.*, 2005, **127**, 2538–2552.

47 W. J. Jang, S. M. Song, J. H. Moon, J. Y. Lee and J. YunCopper-Catalyzed, Enantioselective Hydroboration of Unactivated 1,1-Disubstituted Alkenes, *J. Am. Chem. Soc.*, 2017, **139**, 13660–13663.

48 W. Su, J. Zhu, Y. Chen, X. Zhang, W. Qiu, K. Yang, P. Yu and Q. Song, Copper-catalysed asymmetric hydroboration of alkenes with 1,2-benzazaborines to access chiral naphthalene isosteres, *Nat. Chem.*, 2024, **16**, 1312–1319.

49 S. J. Geier, C. M. Vogels, J. A. Melanson and S. A. Westcott, The transition metal-catalysed hydroboration reaction, *Chem. Soc. Rev.*, 2022, **51**, 8877–8922.

50 Y. Quan and Z. Xie, Controlled functionalization of o-carborane *via* transition metal catalyzed B–H activation, *Chem. Soc. Rev.*, 2019, **48**, 3660–3673.

51 L. Chen and S. J. S. Xu, Ligand-Enabled Regio-and/or Stereoselective Hydroboration of Alkenes, *Synlett*, 2023, **34**, 2103–2109.

52 R. Bisht, C. Haldar, M. M. M. Hassan, M. E. Hoque, J. Chaturvedi and B. Chattopadhyay, Metal-catalysed C–H bond activation and borylation, *Chem. Soc. Rev.*, 2022, **51**, 5042–5100.

53 Q.-Q. Cheng, S.-F. Zhu, Y.-Z. Zhang, X.-L. Xie and Q.-L. Zhou, Copper-Catalyzed B–H Bond Insertion Reaction: A Highly Efficient and Enantioselective C–B Bond-Forming Reaction with Amine–Borane and Phosphine–Borane Adducts, *J. Am. Chem. Soc.*, 2013, **135**, 14094–14097.

54 X. Li and D. P. Curran, Insertion of Reactive Rhodium Carbenes into Boron–Hydrogen Bonds of Stable N-Heterocyclic Carbene Boranes, *J. Am. Chem. Soc.*, 2013, **135**, 12076–12081.

55 A. Yamamoto and M. Suginome, Nickel-Catalyzed trans-Alkynylboration of Alkynes *via* Activation of a Boron−Chlorine Bond, *J. Am. Chem. Soc.*, 2005, **127**, 15706–15707.

56 T. Furukawa, M. Tobisu and N. Chatani, Nickel-catalyzed borylation of arenes and indoles *via* C–H bond cleavage, *Chem. Commun.*, 2015, **51**, 6508–6511.

57 C. F. Meng, B. B. Zhang, Q. Liu, K. Q. Chen, Z. X. Wang and X. Y. Chen, Achieving Nickel-Catalyzed Reductive C(sp(2))-B Coupling of Bromoboranes *via* Reversing the Activation Sequence, *J. Am. Chem. Soc.*, 2024, **146**, 7210–7215.

58 L. Tendera, F. Fantuzzi, T. B. Marder and U. Radius, Nickel boryl complexes and nickel-catalyzed alkyne borylation, *Chem. Sci.*, 2023, **14**, 2215–2228.

59 C.-L. Ji, H. Chen, Q. Gao, J. Han, W. Li and J. Xie, Dinuclear gold-catalyzed divergent dechlorinative radical borylation of gem-dichloroalkanes, *Nat. Commun.*, 2024, **15**, 3721.

60 H. Lyu, I. Kevlishvili, X. Yu, P. Liu and G. Dong, Boron insertion into alkyl ether bonds *via* zinc/nickel tandem catalysis, *Science*, 2021, **372**, 175–182.

61 X. Yang, C. Yuan and S. Ge, Ligand-enabled stereodivergence in nickel-catalyzed regioselective hydroboration of internal allenes, *Chem*, 2023, **9**, 198–215.

62 Z.-L. Chen, C. Empel, K. Wang, P.-P. Wu, B.-G. Cai, L. Li, R. M. Koenigs and J. Xuan, Enabling Cyclopropanation Reactions of Imidazole Heterocycles *via* Chemoselective Photochemical Carbene Transfer Reactions of NHC-Boranes, *Org. Lett.*, 2022, **24**, 2232–2237.

63 W. Srimontree, L. Guo and M. Rueping, Hydride Transfer Enables the Nickel-Catalyzed ipso-Borylation and Silylation of Aldehydes, *Chem. Eur. J.*, 2020, **26**, 423–427.

64 J. Hu, M. Ferger, Z. Shi and T. B. Marder, Recent advances in asymmetric borylation by transition metal catalysis, *Chem. Soc. Rev.*, 2021, **50**, 13129–13188.

65 S. K. Bose, L. Mao, L. Kuehn, U. Radius, J. Nekvinda, W. L. Santos, S. A. Westcott, P. G. Steel and T. B. Marder, First-Row d-Block Element-Catalyzed Carbon-Boron Bond Formation and Related Processes, *Chem. Rev.*, 2021, **121**, 13238–13341.

66 T. Y. Peng, F. L. Zhang and Y. F. Wang, Lewis Base-Boryl Radicals Enabled Borylation Reactions and Selective Activation of Carbon-Heteroatom Bonds, *Acc. Chem. Res.*, 2023, **56**, 169–186.

67 X. Wang, P. Zhang, Z. Yang, W. Sun, H. Lyu, Z. Lin and Y. Quan, Synthesis of strained, air-stable boracycles *via* boron-carbon-centred diradicals, *Nat. Chem.*, 2025, **17**, 663–671.

68 Z. Zhu, W. C. Chan, B. Gao, G. Hu, P. Zhang, Y. Fu, K. S. Ly, Z. Lin and Y. Quan, Borenium-Catalyzed "Boron Walking" for Remote Site-Selective Hydroboration, *J. Am. Chem. Soc.*, 2025, **147**, 880–888.

69 H. C. Johnson, C. L. McMullin, S. D. Pike, S. A. Macgregor and A. S. Weller, Dehydrogenative Boron Homocoupling of an Amine-Borane, *Angew. Chem., Int. Ed.*, 2013, **52**, 9776–9780.

70 Q. Wang, S. E. Motika, N. G. Akhmedov, J. L. Petersen and X. Shi, Synthesis of Cyclic Amine Boranes through Triazole-Gold(I)-Catalyzed Alkyne Hydroboration, *Angew. Chem., Int. Ed.*, 2014, **53**, 5418–5422.

71 K. B. Kolpin and D. J. H. Emslie, η^3-Vinylborane Complexes of Platinum and Nickel: Borataallyl- and Alkyl/Borataalkene-Like Coordination Modes, *Angew. Chem., Int. Ed.*, 2010, **49**, 2716–2719.

72 D. J. H. Emslie, B. E. Cowie and K. B. Kolpin, Acyclic boron-containing π-ligand complexes: η^2- and η^3-coordination modes, *Dalton Trans.*, 2012, **41**, 1101–1117.

73 S. Gomosta, K. Saha, U. Kaur, K. Pathak, T. Roisnel, A. K. Phukan and S. Ghosh, Hydroboration of Alkynes: η^4-Alkene–Borane *versus* η^4-E-Boratabutadiene, *Inorg. Chem.*, 2019, **58**, 9992–9997.

74 Y. Kawano, T. Yasue and M. Shimoi, BH Bond Activation of Trimethylphosphineborane by Transition Metal Complexes: Synthesis of Metal Complexes Bearing Nonsubstituted Boryl−Trimethylphosphine, $Cp^*M(CO)_3(BH_2 \cdot PMe_3)$ (M = Mo, W), *J. Am. Chem. Soc.*, 1999, **121**, 11744–11750.

75 K. Saha, D. K. Roy, R. D. Dewhurst, S. Ghosh and H. Braunschweig, Recent Advances in the Synthesis and Reactivity of Transition Metal σ-Borane/Borate Complexes, *Acc. Chem. Res.*, 2021, **54**, 1260–1273.

76 H. Tao and H. Lyu, Functionalization of Boranes through Thiol/Oxygen Catalysis, *Chin. J. Chem.*, 2024, **42**, 2804–2810.

77 C. Zhu, J. Dong, X. Liu, L. Gao, Y. Zhao, J. Xie, S. Li and C. Zhu, Photoredox-Controlled beta-Regioselective Radical Hydroboration of Activated Alkenes with NHC-Boranes, *Angew. Chem., Int. Ed.*, 2020, **59**, 12817–12821.

78 P. J. Xia, D. Song, Z. P. Ye, Y. Z. Hu, J. A. Xiao, H. Y. Xiang, X. Q. Chen and H. Yang, Photoinduced Single-Electron Transfer as an Enabling Principle in the Radical Borylation of Alkenes with NHC-Borane, *Angew. Chem., Int. Ed.*, 2020, **59**, 6706–6710.

79 F. X. Li, X. Wang, J. Lin, X. Lou, J. Ouyang, G. Hu and Y. Quan, Selective multifunctionalization of N-heterocyclic carbene boranes *via* the intermediacy of boron-centered radicals, *Chem. Sci.*, 2023, **14**, 6341–6347.

80 G. Li, G. Huang, R. Sun, D. P. Curran and W. Dai, Regioselective Radical Borylation of alpha,beta-Unsaturated Esters and Related Compounds by Visible Light Irradiation with an Organic Photocatalyst, *Org. Lett.*, 2021, **23**, 4353–4357.

81 G. Liu and Y. Wu, in *C-H Activation*, ed. J.-Q. Yu and Z. Shi, Springer Berlin Heidelberg, Berlin, Heidelberg, 2010, pp. 195–209, DOI: **10.1007/128_2009_16**.

82 P.-S. Wang and L.-Z. Gong, Palladium-Catalyzed Asymmetric Allylic C–H Functionalization: Mechanism, Stereo- and Regioselectivities, and Synthetic Applications, *Acc. Chem. Res.*, 2020, **53**, 2841–2854.

83 J. S. Bair, Y. Schramm, A. G. Sergeev, E. Clot, O. Eisenstein and J. F. Hartwig, Linear-selective hydroarylation of unactivated terminal and internal olefins with trifluoromethyl-substituted arenes, *J. Am. Chem. Soc.*, 2014, **136**, 13098–13101.

84 S. Tang, O. Eisenstein, Y. Nakao and S. Sakaki, Aromatic C–H σ-Bond Activation by Ni0, Pd0, and Pt0 Alkene Complexes: Concerted Oxidative Addition to Metal *vs.* Ligand-to-Ligand H Transfer Mechanism, *Organometallics*, 2017, **36**, 2761–2771.

85 Z. Ye, C. Y. Kwok, S. L. Lam, L. Wu and H. Lyu, Copper-Catalyzed C-B(sp(3)) Bond Formation through the Intermediacy of Cu-B(sp(3)) Complex, *J. Am. Chem. Soc.*, 2025, **147**, 14915–14923.

86 J. C. Lo, J. Gui, Y. Yabe, C. M. Pan and P. S. Baran, Functionalized olefin cross-coupling to construct carbon-carbon bonds, *Nature*, 2014, **516**, 343–348.

87 J. Zheng, J. Qi and S. Cui, Fe-Catalyzed Olefin Hydroamination with Diazo Compounds for Hydrazone Synthesis, *Org. Lett.*, 2016, **18**, 128–131.